Qualitative theory of rubber friction and wear

B. N. J. Persson
Institut für Festkörperforschung, Forschungszentrum Jülich, D-52425 Jülich, Germany

E. Tosatti
SISSA, Via Beirut 4, I-34014, Trieste, Italy

(Received 28 July 1999; accepted 29 October 1999)

When rubber is slid on a hard, rough substrate, the surface asperities of the substrate exert oscillating forces on the rubber surface leading to energy ''dissipation'' via the internal friction of the rubber. We present a qualitative discussion of how the resulting friction force depends on the nature of the surface roughness and comment on the origin of the wear of sliding rubber surfaces. © *2000 American Institute of Physics.* [S0021-9606(00)51404-4]

I. INTRODUCTION

The nature of the friction when rubber is slid on a hard substrate is a topic of considerable practical importance, e.g., for the construction of tires and wiper blades.[1] Rubber friction differs in many ways from the frictional properties of most other solids. The reason for this is the very low elastic modulus of rubber and the high internal friction exhibited by rubber in a wide frequency region.

The pioneer studies of Grosch[2] have shown that rubber friction in many cases is directly related to the internal friction of the rubber. Thus experiments with rubber surfaces sliding on silicon carbide paper and glass surfaces give friction coefficients with the same temperature dependence as that of the complex elastic modulus $E(\omega)$ of the rubber. In particular, there is a marked change in friction at high speeds and low temperatures, where the rubber's response is driven into the so-called glassy region. In this region, the friction shows marked stick-slip and falls (in spite of increased wear, see Sec. IV) to a level of $\mu \approx 0.4$, which is more characteristic of plastics. This proves that the friction force under most normal circumstances is directly related to the internal friction of the rubber, i.e., it is mainly a *bulk property* of the rubber.[2]

The friction force between rubber and a rough (hard) surface has two contributions commonly described as the adhesion and hysteric components, respectively.[1] The hysteric component result from the internal friction of the rubber: during sliding the asperities of the rough substrate exert oscillating forces on the rubber surface leading to cyclic deformations of the rubber and to energy ''dissipation'' via the internal damping of the rubber. This contribution to the friction force will therefore have the same temperature dependence as that of the elastic modulus $E(\omega)$ (a bulk property). The adhesion component is important only for very clean surfaces.

Because of its low elastic modulus, rubber often exhibit elastic instabilities during sliding. The most well-known involves the compressed rubber surface in front of the contact area undergoing a buckling which produces detachment waves which propagate from the front-end to the back-end of the contact area. These so-called Schallamach waves[3] occur mainly at ''high'' sliding velocity for very smooth surfaces and will not be considered further in this paper.

In an earlier paper one of the present authors has studied both the adhesion and hysteric components of rubber friction.[4,5] Other studies of this topic are presented in Refs. 1 and 6–8. Reference 4 considered only the interaction between a flat rubber surface and a single surface asperity (or many identical asperities). In the present paper we present a more complete treatment of the hysteric contribution to the friction for viscoelastic solids sliding on hard substrates with different types of (idealized) surface roughness. We note, however, that rubber friction is a very complex topic, and the present study is of a semiquantitative nature, with the main aim being to understand the qualitative role of surface roughness on rubber friction.

II. AREA OF REAL CONTACT: QUALITATIVE DISCUSSION

Consider a flat rubber surface squeezed against a hard surface with a periodic corrugation with wavelength λ and amplitude (or height) h; see Fig. 1. If A is the area of the rubber surface and L the load, then we define the average perpendicular stress (or pressure) $\sigma_0 = L/A$. Let us now study under which conditions the load L, and the rubber-substrate adhesion forces, are able to deform the rubber so that it comes in direct contact with the substrate over the *whole* surface area [Fig. 1(b)], i.e., under which conditions the rubber is able to fill out all the surface ''cavities'' of the substrate.

Assume first that a uniform stress σ acts within a circular area (radius R) centered at a point P on the surface of a semi-infinite elastic body with the elastic modulus E. This will give rise to a perpendicular displacement u of P by a distance which is easy to calculate using continuum mechanics: $u/R \approx \sigma/E$. This result can also be derived from simple dimensional arguments: First, note that u must be proportional to σ since the displacement field is linearly related to the stress field (we assume here, and in what follows, that the strain is so small that linear elasticity theory is valid). However, the only other quantity in the problem with the same dimension as the stress σ is the elastic modulus E so u must

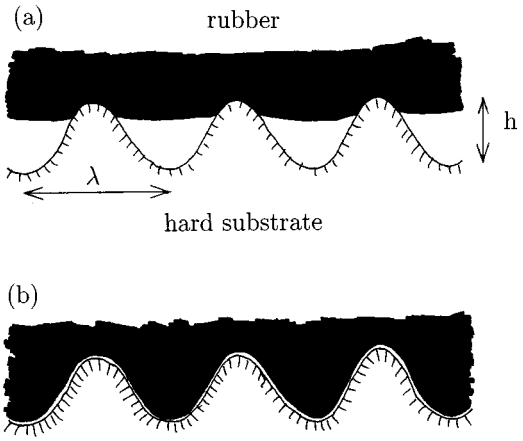

FIG. 1. (a) A flat rubber surface sliding on a hard corrugated substrate. In (b) the perpendicular pressure, or the rubber-substrate adhesion, is able to deform the rubber so as to completely follow the corrugated substrate profile.

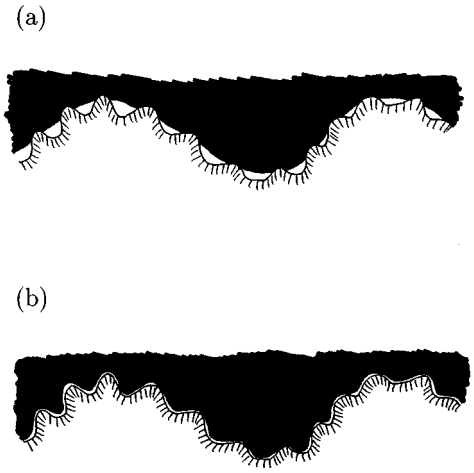

FIG. 2. (a) At ''high'' sliding velocity the rubber is not able to follow the short-wavelength substrate profile because of the increase in the stiffness of the rubber at high perturbing frequencies. (b) At ''low'' sliding velocity the rubber is able to fill out also the small-sized substrate cavities.

be proportional to σ/E. Since R is the only quantity with the dimension of length we get at once $u\sim(\sigma/E)R$. Thus, with reference to Fig. 1, if $h/\lambda\approx\sigma_0/E$, the perpendicular pressure σ_0 will be just large enough to deform the rubber to make contact with the substrate everywhere.

Next, let us consider the role of the rubber-substrate adhesion interaction. When the rubber deforms and fills out a surface cavity of the substrate, an elastic energy $E_{\rm el}\approx E\lambda h^2$ will be stored in the rubber. Now, if this elastic energy is smaller than the gain in adhesion energy $E_{\rm ad}\approx\Delta\gamma\lambda^2$ as a result of the rubber-substrate interaction (which usually is mainly of the van der Waals type), then (even in the absence of the load L) the rubber will deform spontaneously to fill out the substrate cavities. The condition $E_{\rm el}=E_{\rm ad}$ gives[4,5] $h/\lambda\approx(\Delta\gamma/E\lambda)^{1/2}$. For the rough surfaces of interest here we typically have $h/\lambda\approx1$, and with $E=1$ MPa and $\Delta\gamma=3$ meV/Å^2 the adhesion interaction will be able to deform the rubber and completely fill out the cavities if $\lambda<1000$ Å. Note that the adhesion interaction is more important than the applied pressure if $\Delta\gamma>\sigma^2\lambda/E$. It will be shown below that the local pressure in a contact area (which is higher than the average pressure σ_0) typically is of order E so that the adhesion interaction dominates if $\Delta\gamma>E\lambda$. With the same parameters as above this gives $\lambda<100$ Å, i.e., the adhesion interaction dominates for nanoscale cavities.

In the case of passenger tires one typically has $\sigma_0\approx0.2$ MPa, and in the case of truck tire 0.8 MPa. This is at least one order of magnitude smaller than the (static) elastic modulus $E\approx10$ MPa of filled rubbers (but only a little smaller than that of unfilled rubber where $E\approx1$ MPa). We conclude that the pressure σ_0 is in general not able to deform the rubber to fill out the large surface cavities on a road, since in this case one typically has $h/\lambda\approx1$, which according to the discussion above would require a local pressure of order $\sigma\approx E$. However, note the following: If the roughness in Fig. 1 represents the largest asperities on a road, then, since road surfaces are nearly fractal (see Sec. III D), the large asperities (or cavities) will have smaller asperities (or cavities) and so on. Now, according to the contact theory of Greenwood (see Sec. III B), the *average* pressure which acts in the rubber-substrate contact area at the *largest* asperities is of order $\sigma\approx(\Delta/R)^{1/2}E$, where Δ is the rms surface roughness amplitude and R the (average) radius of curvature of the large surface asperities. Since for a road surface we expect $\Delta\approx R$ it is clear that the local pressure in the contact area of the large surface asperities will be of order of E, i.e., just large enough in order for the rubber to deform and *fill out the smaller surface cavities*.

The discussion above is for stationary surfaces. During sliding we must take into account that the elastic modulus E depends on the perturbing frequency ω, and that $E(\omega)$ is a complex quantity with an imaginary part related to the internal friction of the rubber. In a first approximation we may still use the estimates presented above if we replace $E=E(0)$ with $|E(\omega)|$ where the frequency $\omega=v/\lambda$. Now, for a typical rubber at room temperature $E(\omega)\approx E(0)$ for $\omega=\omega_c<10^5\ {\rm s}^{-1}$. For higher frequencies $|E(\omega)|$ increases rapidly [see Fig. 4(a)]. This has the following important implications: For asperities (or cavities) with linear size $\lambda>v/\omega_c$ the local stress $\sigma\approx E(0)$ so that the rubber can deform and completely follow the substrate corrugation. In a typical case, for a tires sliding on a road with $v\approx10$ m/s one gets $v/\omega_c\approx0.1$ mm. Thus in this case the rubber is able to deform and fill out only the very long wavelength surface roughness ($\lambda>0.1$ mm); see Fig. 2(a). On the other hand, in Anti-Lock Braking System (ABS) of automobile tires on dry or wet road $v<1$ cm/s in the incipient part of the footprint area, and in this case $v/\omega_c<1000$ Å so that all surface cavities with linear size larger than 1000 Å will be filled out by the rubber [Fig. 2(b)]. Whether the nanoscale cavities will be filled out by the rubber depends on the magnitude of the surface energy and of $|E(\omega)|$ evaluated for $\omega\sim v/\lambda$ (where λ is the size of the nanoscale asperity or cavity).

The following observation may also be relevant for the question of whether the small sized (nanoscale) substrate cavities can be filled out by the rubber: Rubber used for tires has fillers (carbon or silica particles) which increases the

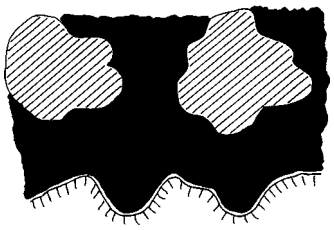

FIG. 3. Rubber with filler particles in contact with a hard substrate with nanocavities.

macroscopic elastic modulus from roughly 10^6 Pa for pure rubber to 10^7 Pa for the composite. However, the filler particles are typically 1000 Å or larger, and will be surrounded by ''pure'' rubber. Since the filler particles, and the average distance between the filler particles in the rubber matrix, typically are larger the than nanoscale cavities (see Fig. 3), it is not appropriate to use the macroscopic elastic modulus when determining whether the rubber will fill out the nanoscale cavities, but rather one should use the elastic modulus of pure rubber, i.e., $E \approx 10^6$ Pa. (If a rubber surface has been standing for some time without use, it may be covered by a thin hardened skin, which results from oxidation or the influence of the sun light; in this case also the hardened layer must be taken into account in the analysis of the role of nanoscale cavities.)

The discussion above refers to clean surfaces. For contaminated surfaces the small-sized surface cavities may be filled by contamination (e.g., by water on a wet road), or the rubber surface may be covered by dust which prevents the rubber from penetrating the small sized cavities; this will reduce the role of the rubber-substrate adhesion and lower the sliding friction.

III. RUBBER FRICTION: ROLE OF THE SURFACE ROUGHNESS

In this section we use the theory of viscoelasticity to estimate the contribution of the surface roughness of the substrate to the friction force when rubber is slid on a hard, rough substrate.

The energy dissipation in a viscoelastic media is in general given by

$$\Delta E = \int d^3x\, dt\, \sigma_{ij} \dot{\varepsilon}_{ij},$$

where σ_{ij} is the stress tensor and ε_{ij} the strain tensor. The dot denotes time derivative. For uniaxial deformations of a cylindrical bar this formula reduces to

$$\Delta E = -\frac{V}{2\pi} \int d\omega\, \omega\, \mathrm{Im}[\sigma(\omega)\varepsilon^*(\omega)]$$

or

$$\Delta E = \frac{V}{2\pi} \int d\omega\, \omega\, \mathrm{Im}\left(\frac{1}{E(\omega)}\right) |\sigma(\omega)|^2$$

$$= -\frac{V}{2\pi} \int d\omega\, \omega\, \frac{\mathrm{Im}\, E(\omega)}{|E(\omega)|^2} |\sigma(\omega)|^2, \qquad (1)$$

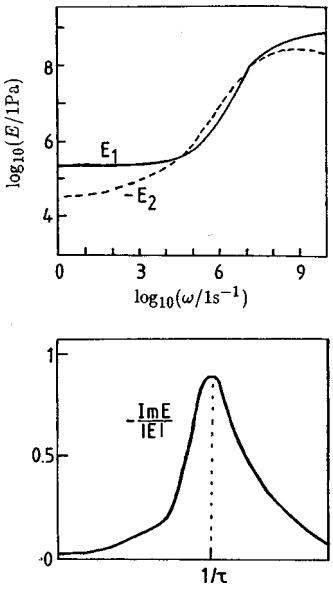

FIG. 4. Typical frequency dependence (for rubber) of (a) the complex elastic modulus $E(\omega)$ and (b) $-\mathrm{Im}\, E(\omega)/|E(\omega)|$.

where V is the volume of the solid. Figure 4(a) shows the real $E_1(\omega)$ and the imaginary part $E_2(\omega)$ of the complex elastic modulus $E = E_1 + iE_2$ of rubber (schematic). Figure 4(b) shows the the function $-\mathrm{Im}\, E(\omega)/|E(\omega)|$. Note that the latter function is maximal for $\omega = 1/\tau$, where τ can be interpreted as the typical time associated with flipping of some segment of a rubber molecule from one configuration to another. Note that the ''flipping'' is a thermally activated process and τ depends exponentially (or faster) on the temperature, $\tau \approx \tau_0 \exp(\epsilon/k_B T)$. In a more accurate description of the dynamical properties of rubber it is necessary to introduce a wide distribution of relaxation times.

We can use the equations above to estimate the contribution from the internal friction to the sliding friction of rubber. In an earlier paper[4] we considered the case of a single contact area (or several identical contact areas). In this work we present a more complete discussion about the role of the nature of the surface roughness.

A. Identical asperities

We consider first the sliding configuration shown in Fig. 5. A viscoelastic body (e.g., rubber) with a flat surface slides with the velocity v on a rigid substrate with periodic ''roughness.'' The sliding motion results in fluctuating stresses acting on the surface of the viscoelastic solid, and characterized

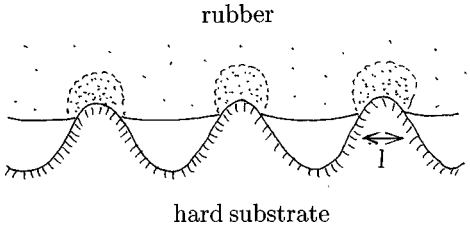

FIG. 5. The fluctuating stress $\sigma(t)$ acting on the surface area $\sim l^2$ gives rise to energy ''dissipation'' via the internal friction of the solid. The main part of the ''dissipation'' occurs in the dotted volume elements $V \sim l^3$.

by the frequency $\omega_0 \sim v/l$, where v is the sliding velocity and l a length of order the diameter of the contact area between a substrate asperity and the rubber surface (see Fig. 5). The main part of the energy ''dissipation'' occur in the dotted volume element (see Fig. 5) $V \sim l^3$. If L is the load (or normal force) then the fluctuating stress acting on the surface area l^2 is $\sigma \sim \sigma_0 \cos \omega_0 t$, where the (average) stress $\sigma_0 = L/Nl^2$, where N is the number of (identical) asperities or contact areas. Substituting this in (1) gives

$$\Delta E \approx N l^3 \sigma_0^2 \omega_0 T \, \mathrm{Im}\left(\frac{1}{E(\omega_0)}\right), \tag{2}$$

where T is the total time the oscillating stress has acted on the solid. We note that the rubber strain field in Fig. 5 is, of course, not the same as in uniaxial deformation of a cylindrical bar as assumed in the derivation of (1). Nevertheless, to within a factor of order unity (which depend on the Poisson ratio $\nu \approx 0.5$) the expression (2) gives the dissipated energy during the time period T. This follows from dimensional arguments, but can also be shown directly from explicit model calculations. The energy dissipation per unit time $\Delta E/T$ must equal the product Fv between the friction force and the sliding velocity so that

$$F \approx N \frac{l^3 \sigma_0^2 \omega_0}{v} \, \mathrm{Im}\left(\frac{1}{E(\omega_0)}\right).$$

Since $L = Nl^2 \sigma_0$ we get

$$\mu = \frac{F}{L} \approx \sigma_0 \, \mathrm{Im}\left(\frac{1}{E(\omega_0)}\right). \tag{3}$$

The average stress σ_0 is given by Hertz contact theory $\sigma_0 \sim E^{2/3}(L/N)^{1/3}$; this introduces a dependence of the friction coefficient on the load L (and on the number of asperities N) which is usually not observed experimentally.

On the other hand, as shown by Greenwood, and discussed in the next section, for surface asperities with random height the average stress σ_0 is nearly independent of the normal force (and on the number of asperities) in agreement with experiments.

B. Nonoverlapping, stochastically varying asperities

Let us now consider a distribution of contact areas with different sizes as indicated in Fig. 6(a). Let $P(l,\sigma)$ be the probability that a contact area has the diameter l and the (average) perpendicular stress σ:

$$\int d\sigma \, dl \, P(l,\sigma) = 1.$$

If the surface asperities are well separated so that we can neglect the interaction between the displacement field in the rubber derived from the different contact areas, then it is easy to generalize the result presented above. The friction force becomes

$$F = N \int d\sigma \, dl \, P(l,\sigma) \frac{l^3 \sigma^2 \omega_l}{v} \, \mathrm{Im}\left(\frac{1}{E(\omega_l)}\right).$$

Since

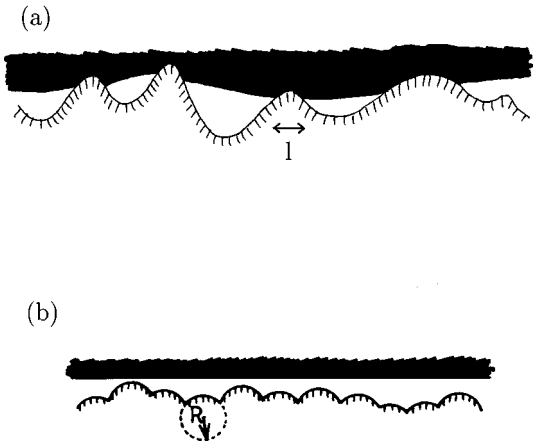

FIG. 6. (a) Rubber sliding on a surface with nonoverlapping surface asperities. (b) The contact model studied by Greenwood, Ref. 9.

$$L = N \int d\sigma \, dl \, P(l,\sigma) l^2 \sigma$$

we get

$$\mu = \frac{F}{L} \approx \frac{\int d\sigma \, dl \, P(l,\sigma) l^2 \sigma^2 \, \mathrm{Im}[1/E(\omega_l)]}{\int d\sigma \, dl \, P(l,\sigma) l^2 \sigma}. \tag{4}$$

This equation is valid under rather general conditions, but we consider now the simplest case where the surface asperities are approximated as spherical cups of identical radius R but of different height, see Fig. 6(b). This model was originally studied by Greenwood[9] in the context of contact mechanics. He showed that the model predict that the area of real contact is (nearly) proportional to the load (and independent of the apparent contact area, e.g., independent of the number of surface asperities), as is usually observed experimentally. Since the radius R is fixed, the contact diameter l and the (average) perpendicular stress σ are not independent parameters but are related to each other via Hertz contact theory: $\sigma = [4E/3\pi(1-\nu^2)](h/R)^{1/2}$ and $l \approx (Rh)^{1/2}$, where h is the distance the rubber is compressed by an asperity. Thus we can replace the probability distribution $P(l,\sigma)$ with $P(h)$ which only depends on h. In many cases the asperity height distribution is nearly Gaussian, and in this case we have (approximately)[5,9] $P(h) = A \exp(-qh)$ where $q = a/\Delta$, where Δ is the rms width of the (Gaussian) asperity height distribution, and where a is a number which depends very weakly on h, but in most cases of interest it can be taken as a constant, $a \approx 2-3$. Substituting these results in (4) and writing $h/\Delta = x$ and $\omega_x = v(xR\Delta)^{-1/2}$ gives

$$\mu \approx \frac{\int_0^\infty dh \, P(h) l^2 \sigma^2 \, \mathrm{Im}[1/E(\omega_l)]}{\int_0^\infty dh \, P(h) l^2 \sigma}$$

$$\approx \frac{4}{3\pi(1-\nu^2)} \left(\frac{\Delta}{R}\right)^{1/2} \frac{\int_0^\infty dx \, x^2 e^{-ax} \, \mathrm{Im} \, E(\omega_x)}{\int_0^\infty dx \, x^{3/2} e^{-ax} |E(\omega_x)|}. \tag{5}$$

In most cases $E(\omega_x)$ varies much slower with x than the prefactor in the integrals above, and we can therefore move $E(\omega_x)$ outside the integral, with ω_x evaluated at the x where the prefactor is maximal, i.e., for $x \approx 1$. This gives

$$\mu \approx -C \frac{\mathrm{Im}\, E(\omega_1)}{|E(\omega_1)|}, \tag{6}$$

where $C \approx (\Delta/R)^{1/2}$ and $\omega_1 \approx v(R\Delta)^{-1/2}$. For very rough surfaces, such as a road surface, we have $\Delta \approx R$ and so $C \approx 1$ and $\omega_1 \sim v/R$. Since $\mathrm{Im}\, E(\omega_0)/|E(\omega_0)| \sim 1$ when $\omega_0 \sim 1/\tau$ [see Fig. 3(b)] one expects the maximum of the coefficient of friction to be of order unity, as is usually observed experimentally.

Note that (6) is of the form (3) with $\sigma_0 = C|E(\omega_1)|$ rather than $\sigma_0 \sim E^{2/3}(L/N)^{1/3}$ as follows from Hertz contact theory. The theory above shows that this is a result of the fact that we have a distribution of asperity heights rather than asperities of identical height. In fact, this result can also be understood from very simple dimensional arguments: In experiments with rubber it is usually found that the friction coefficient μ is (nearly) independent of the normal force or load L. (This is not true when the load L is very small or very large. In the former case, adhesion between the rubber and the substrate becomes important. In the latter case, the area of real contact approaches the apparent area of contact, and the area of real contact cannot increase linearly with the load.) This is the case, for example, in the experiments by Grosch[2] and by Mori *et al.*[10] Since no plastic deformation is assumed to occur in the context of rubber friction, the elastic modulus E is the *only* quantity in the problem with the same unit as pressure, and it follows immediately that $\sigma_0 = CE$, i.e., *dimensional analysis alone predicts that the (average) pressure in the areas of real contact is proportional to the elastic modulus E of the rubber*, where C (which may be larger or smaller than unity) depends only on the nature of the surface roughness [in the Greenwood theory, $C \approx (\Delta/R)^{1/2}$, see above]. For sliding surfaces $E(\omega_0)$ is complex, and we will assume that $\sigma_0 \approx C|E(\omega_0)|$. Note that σ_0 depends on the sliding velocity v: increasing v leads to a stiffening of the elastic properties and (for a given load) to a reduced contact area, and to an increased surface stress σ_0 in the contact areas.

The study presented above can be generalized to include a distribution of curvature radii $\{R_i\}$, corresponding to different asperity sizes. If we assume that all the different sized asperities have the same probability height distribution, then we get

$$\mu \approx -\sum_i C_i g_i \frac{\mathrm{Im}\, E(\omega_i)}{|E(\omega_i)|}, \tag{7}$$

where

$$g_i = \frac{f_i |E(\omega_i)| (R_i/\Delta)^{1/2}}{\Sigma_j f_j |E(\omega_j)| (R_j/\Delta)^{1/2}}, \tag{8}$$

where f_i is the fraction of the asperities of type (size) ''*i*.'' Note that $\Sigma_i g_i = 1$. If the distribution of asperity sizes is wide, as is usually the case in practical applications, it will broaden the function $\mu(v)$ and reduce its maximum. This effect may be of practical importance, but contains no new interesting physics and will not be considered further in this paper.

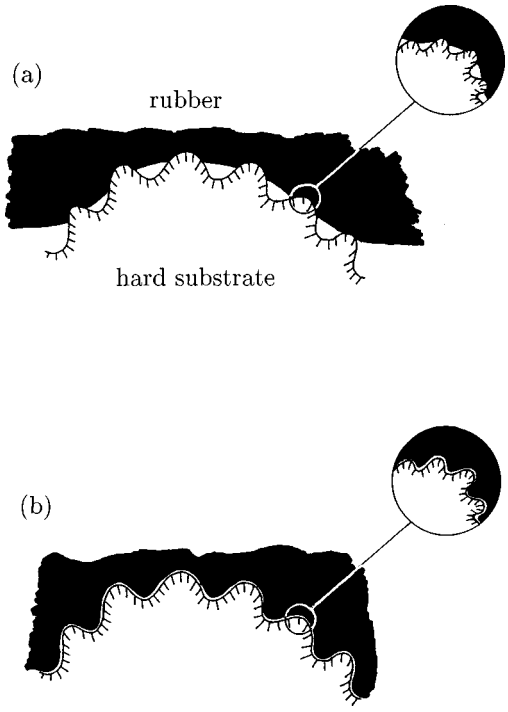

FIG. 7. A surface with large asperities and overlapping small asperities. In (a) the rubber is not able to fill out the small ''cavities,'' while it is able to do so in (b).

C. Overlapping asperities

Many real surfaces can be approximated as fractal (or, more accurately, self-affine fractal, see Sec. III D) in some (finite) roughness-size interval. A fractal surface is characterized by having ''overlapping'' surface asperities. With this we mean that ''large'' surface asperities are covered by ''small'' asperities, and the ''small'' asperities are covered by even smaller asperities and so on (see Fig. 7). We will now show that in this case the function $\mu(v)$ broadens, but the peak maximum *does not decrease* as would be the case for nonoverlapping surface asperities of different sizes (see Sec. III B). Let us first consider the situation illustrated in Fig. 7. We assume only two types of asperities, namely large (radius of curvature R_0) asperities covered by small (radius of curvature R_1) asperities. Even though the displacement fields in the rubber associated with a large asperity overlap with the displacement field of the small asperities, when calculating the energy dissipation we can simply add the two contributions since they involve *different loss frequencies* and are therefore additive. Assume first that the rubber is *not* able to deform and completely fill out the small cavities as illustrated in Fig. 7(a). The energy dissipation induced by the large asperities occurs (mainly) in the volume element l_0^3. The energy dissipation associated with small asperities occurs (mainly) in the volume element l_1^3. If we assume that for each ''large'' asperity, there are N_1 ''small'' asperities in contact with the sliding solid, then the energy dissipation (for each large asperity):

$$\Delta E \approx l_0^3 \sigma_0^2 \omega_0 T\, \mathrm{Im}\left(\frac{1}{E(\omega_0)}\right) + N_1 l_1^3 \sigma_1^2 \omega_1 T\, \mathrm{Im}\left(\frac{1}{E(\omega_1)}\right).$$

Now, note that

$$L=\sigma_0 l_0^2=N_1\sigma_1 l_1^2.$$

Using this equation gives

$$\mu=\frac{F}{L}\approx\sigma_0\,\mathrm{Im}\left(\frac{1}{E(\omega_0)}\right)+\sigma_1\,\mathrm{Im}\left(\frac{1}{E(\omega_1)}\right), \tag{9}$$

where $\omega_0=v/l_0$ and $\omega_1=v/l_1$. As before we may write $\sigma_0=C_0|E(\omega_0)|$ and $\sigma_1=C_1|E(\omega_1)|$, where C_1 is given in the Appendix. We note that the analysis presented above is approximate in that the ''load'' on the ''small'' asperities in Fig. 7(a) are not identical (and equal to L/N_1) as assumed above, but it depends on the distance r of the asperity away from the center of the Hertzian contact area between the big asperity and the substrate (it is proportional to $[1-(r/r_0)^2]^{1/2}$, where r_0 is the radius of the contact area). However, this effect can be taken into account in the analysis: the main result is that it will lead to some additional broadening of the function $\mu(v)$ (see the Appendix).

Next, let us assume that the rubber is able to completely fill out the small cavities, as illustrated in Fig. 7(b); as discussed in Sec. II this case is expected in most practical situations. In this case we can estimate the energy dissipation derived from the small cavities as follows. To deform the rubber to fill out a cavity of width λ and depth h requires the stress (see Sec. II) $\sigma_1\approx|E(\omega_1)|h/\lambda$ (where $\omega_1=v/\lambda$) acting on the area λ^2. Thus the N_1 small cavities will give rise to the energy dissipation

$$N_1\lambda^3\sigma_1^2\omega_1 T\,\mathrm{Im}\left(\frac{1}{E(\omega_1)}\right)=N_1|E(\omega_1)|^2h^2vT\,\mathrm{Im}\left(\frac{1}{E(\omega_1)}\right)$$

which gives the following contribution to the friction force:

$$N_1|E(\omega_1)|^2h^2\,\mathrm{Im}\left(\frac{1}{E(\omega_1)}\right).$$

The contribution to the friction coefficient is obtained by dividing this force with the load $N_1\lambda^2\sigma_0$:

$$\left(\frac{h}{\lambda}\right)^2\frac{\mathrm{Im}\,E(\omega_1)}{\sigma_0}.$$

Using $\sigma_0=C_0|E(\omega_0)|$ the total friction coefficient equals

$$\mu\approx C_0\frac{\mathrm{Im}\,E(\omega_0)}{|E(\omega_0)|}+C_1\frac{\mathrm{Im}\,E(\omega_1)}{|E(\omega_1)|}, \tag{10}$$

where

$$C_1=\frac{1}{C_0}\left(\frac{h}{\lambda}\right)^2\frac{|E(\omega_1)|}{|E(\omega_0)|}\approx\left(\frac{R}{\Delta}\right)^{1/2}\left(\frac{h}{\lambda}\right)^2\frac{|E(\omega_1)|}{|E(\omega_0)|}. \tag{11}$$

The analysis presented above can be extended to the case where the ''small'' asperities in Fig. 7 are covered by even smaller asperities and so on. Thus, in general we get

$$\mu\approx\sum_i C_i\frac{\mathrm{Im}\,E(\omega_i)}{|E(\omega_i)|}. \tag{12}$$

D. Self-affine fractal surfaces

It has been found that many ''natural'' surfaces, e.g., surfaces of stones generated by fracture, can be approximately described as fractal, or, more accurately, as ''self-affine'' surfaces, over a rather wide roughness size region. A self-affine surface has the property that if we make a scale change that is different for each direction, then the surface do not change its morphology. Recent studies have shown that asphalt road tracks are (approximately) self-affine in a finite surface roughness interval, with an upper cutoff at about 1 mm.

In order to study rubber friction on a hard self-affine surface, it is first necessary to be able to describe the contact mechanics. The model described in Sec. III C is an example of the contact between a flat rubber surface and a hard self-affine surface, for the particular case where the scale change is the same in each direction (i.e., a fractal surface), and the contact mechanics for this case was worked out already 1957 by Archard.[11] He showed that the area of real contact is directly proportional to the load (or normal force), $\Delta A\sim L$. In a recent series of papers by Bhushan and co-workers,[12] it is claimed that for self-affine surfaces the area of real contact depends nonlinearly on the load, $\Delta A\sim L^{2(4-D)}$, where D is the fractal dimension of the surface. Since $D>2$ ($D=2$ correspond to a flat surface), this theory predicts that the area of real contact increases faster than linear with the load. This is usually not observed experimentally. In our opinion, the theory of Bhushan and co-workers is based on some questionable assumptions, and we will therefore base the following discussion on the picture of Archard.

When the picture of Archard is valid, the friction coefficient is given (approximately) by (12). The sum in (12) is over different length scales. The subdivision of the surface profile into a hierarchy of length scales depend on the particular surface under study. Now in most cases the upper limit in the sum is quite obvious. For example, for an asphalt road track the upper cutoff is of order 1 mm (the typical grain size) as observed in surface profile measurements. In a recent measurement an asphalt road was observed to by self-affine down to the shortest length-scale studied (approximately 0.03 mm). The low length scale cutoff in the sum (12) is, however, usually not determined by the intrinsic cutoff of the fractal nature of the surface (which may be an atomic distance), but (for clean surfaces) by the mechanisms discussed in Sec. II. For contaminated surfaces the low-distance cutoff may be determined by the nature of the contamination. For example, if the rubber surface is covered by small (uniformly sized) dust particles (e.g., talk or carbon or silica particles from the fillers, or pulverized stone from a road) then the low distance cutoff is obviously determined by the particle size. On the other hand, if the surface is covered by water or some other ''lubrication'' liquid (e.g., oil or grease), which fills out the small surface cavities, then the low distance cutoff will be determined by the smallest asperities which can penetrate above the contamination layer. In any case, the contamination layer will remove the contribution to the energy dissipation from the small surface asperities and cavities, and reduce the friction force.

IV. RUBBER WEAR

Let us briefly discuss wear in the context of rubber friction. When a block of rubber is exposed to low-frequency

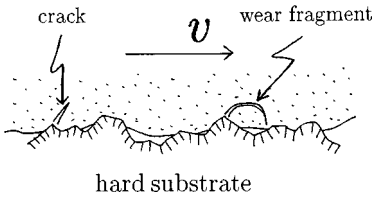

FIG. 8. Wear of rubber at high sliding velocity v on a hard, rough, substrate. The wear result from the small-sized surface asperities which generate pulsating forces with frequencies in the glassy region of the rubber loss spectra.

shear stresses at room temperature the rubber response is elastic, and there is likely to be very small wear. However, strong wear may occur at low temperatures, or at very high frequencies, where the rubber behave as a glassy brittle material. Thus at low temperature rubber can fracture by crack propagation (recall the Challenger catastrophe) as there is no time for the rubber molecule to deform elastically by thermal excitation over the energy barriers.[13] Similarly, at high enough frequency the rubber will respond in a glassy brittle manner even at room temperature.[13] Now, when a rubber block is sliding on a rough surface with roughness on many different length scales (fractal surface), the very small surface asperities will generate very high-frequency pulsating forces on the rubber surface: $\omega_l \sim v/l$, where l is the linear size of a contact area. At room temperatures most types of rubber will be in the glassy state when $\omega > 10^8 - 10^9\ \mathrm{s}^{-1}$. If we consider the sliding velocity $v \sim 10$ m/s (typical for a wheel during breaking on a road) this gives brittle or glassy response for $l < 100-1000$ Å. Thus one expects in this case large wear, with rubber particles of linear sizes $\sim 100-1000$ Å being removed (by brittle fracture) during breaking, see Fig. 8. This estimate assumes that the rubber surface does not heat up to any great extend as a result of the frictional energy dissipation. This assumption may only hold at the initial phase during emergency breaking (locked wheels): for sliding at high velocity during a ''long'' time period the rubber surface temperature may become so high that the rubber does not behave as a glassy solid even when exposed to fluctuating stresses in the frequency range $\omega_l \sim 10^9 - 10^{10}\ \mathrm{s}^{-1}$. Based on the Williams–Landel–Ferry equation one can estimate that a temperature increase from 300 K (room temperature) to 330 K gives approximately an order of magnitude shift of the glassy region to higher frequencies.

The situation is different for slowly sliding rubbers. Thus when $v < 1$ cm/s, as is the case for the extremely important application to ABS-braking of automotive tires on dry or wet road surfaces (where $v \sim 0.01-1$ cm/s in the incipient part of the footprint area), then the rubber will be able to deform and fill out the nanoscale cavities associated with the short-ranged surface roughness. This leads to an increased friction coefficient but small wear, since the relevant frequencies v/l are well below those corresponding to the glassy brittle region of most rubbers.

The discussion above is in agreement with experimental data. Figure 9 shows the temperature dependence of the wear and the friction when rubber is slid on a hard rough substrate at a fixed velocity. Note first that the friction is small at high

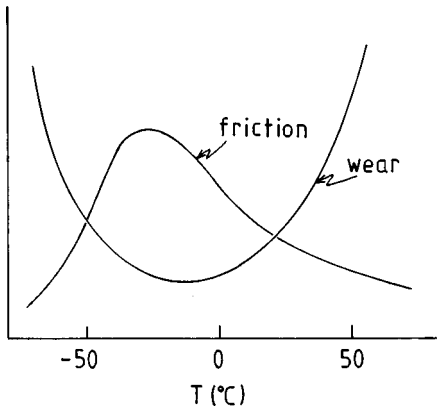

FIG. 9. The temperature dependence of the wear and the friction coefficient for rubber sliding on a rough hard substrate at a fixed velocity (schematic). The figure is based on experimental results of A. Schallamach, Rubber Chem. Technol. **209**, 95 (1968).

temperature where, at the relevant frequencies $\omega_l = v/l$ associated with the asperity-rubber interaction, the rubber is in the rubbery region of the viscoelastic response and where the loss function $\mathrm{Im}\, E(\omega_l)/|E(\omega_l)|$ is small. When the temperature is reduced, the friction initially increases and reaches a maximum when the perturbing frequencies ω_l are located in the transition region between the rubbery region and the glassy region, where $\mathrm{Im}\, E(\omega_l)/|E(\omega_l)|$ is maximal. Finally, when the temperature is reduced below ~ -40 °C the friction coefficient decreases as ω_l now moves into the glassy region where $\mathrm{Im}\, E(\omega_l)/|E(\omega_l)|$ is small. Thus, from the discussion above we expect the wear to increase when T is reduced below -40 °C as is indeed observed experimentally (see Fig. 9). Note, however, that the wear also increases at high temperatures. This can be understood as follows. During sliding the asperities exert (oscillating) shear stresses on the rubber, but in the rubbery region this stress is by itself usually not large enough to break the strong covalent bonds (e.g., the sulphur bonds) in the rubber. However, at high enough temperatures thermal fluctuations may break a bond, in particular if it is already stretched as a result of the external stress. This stress-aided thermally activated bond-breaking will give rise to a rapid increase in the wear at high temperatures. Thus, we expect the temperature-dependence of the wear to have the U-shaped form shown in Fig. 9. Note also that the wear is minimal close to the point where the friction is maximal. Thus, as is now well known, there is no simple relation between wear and friction and, in particular, a large friction coefficient does not necessarily imply a large wear.

Other wear processes discussed in the literature involve the influence of sun light and oxidation on the rubber surface, leading to a thin hardened and brittle surface layer which may be removed relatively easily by the stresses the rubber surface is exposed to under its practical use.

V. SUMMARY

There is at present a strong drive by tire companies to design new rubber compounds with lower rolling resistance, higher sliding friction and reduced wear. At present these

attempts are mainly based on a few empirical rules and on very costly trial-and-error procedures. We believe that a fundamental understanding of rubber friction and wear may help in the design of new rubber compounds for tires and other rubber applications, e.g., wiper blades.

In the present paper we have discussed the factors which determine the area of real contact between a rubber block and a hard rough surface. We have shown that for stationary surfaces (or low sliding velocity) for typical pressures in the (apparent) contact area between a car tire and a asphalt road the rubber will only make contact with about 5% of the large road surface asperities (which are associated with the upper cutoff length in the fractal distribution of the substrate surface roughness). However, in each such contact area the local pressure is large enough to squeeze the rubber into the smaller-sized ''cavities.''

We have studied the sliding friction for rubber on surfaces with different types of (idealized) surface roughness. In general, the friction coefficient $\mu=\Sigma_i C_i \,\mathrm{Im}\, E(\omega_i)/|E(\omega_i)|$, where $E(\omega)$ is the complex elastic modulus evaluated at the frequency ω, and where the sum is over the different surface roughness length scales λ_i, with $\omega_i=v/\lambda_i$ and where C_i depend on the nature of the surface roughness (e.g., the ratio of the amplitude to the wavelength of the surface roughness profile). The detailed dependence of C_i on the parameters which characterizes self-affine fractal surfaces has not been studied in the present paper, and remain as a very important topic for future studies of rubber friction (see also Ref. 8). Finally, we have given some arguments about the origin of the wear of rubber surfaces at low and high temperatures.

ACKNOWLEDGMENTS

B.P. would like to thank G. Heinrich for useful discussions and for drawing his attention to the fascinating field of rubber friction. He also thank BMBF for a grant related to the German–Israeli Project Cooperation ''Novel Tribological Strategies from the Nano-to-Meso-Scales.''

APPENDIX

Let us consider a ''large'' asperity with radius of curvature R_0. The radius of the Hertzian contact region when the asperity is squeezed against a substrate is denoted by r_0. In the contact region (area $A_0=\pi r_0^2$) we assume N_1 smaller asperities (radius R_1) with the concentration $n=N_1/A_0=1/a^2$ where the last equation define the length a. Using Hertz contact theory we get

$$A_0=\pi r_0^2=R_0 h_0,$$

where h_0 is the distance the big surface asperity is compressed. The stress in the contact region is given by

$$\sigma(r)=\sigma_0\frac{3}{2}\left(1-\frac{r^2}{r_0^2}\right)^{1/2},$$

where

$$\sigma_0=\frac{4E_0}{3\pi(1-\nu^2)}\left(\frac{h_0}{R_0}\right)^{1/2},$$

where $E_0=|E(\omega_0)|$. The small asperity at a distance r from the center experience a load

$$L_1=a^2\sigma_0\frac{3}{2}\left(1-\frac{r^2}{r_0^2}\right)^{1/2}$$

and the stress

$$\sigma_1=\frac{L_1}{\pi r_1^2}=\frac{a^2\sigma_0}{\pi r_1^2}\frac{3}{2}\left(1-\frac{r^2}{r_0^2}\right)^{1/2}.$$

Furthermore, since from Hertz contact theory [with $E_1=E(\omega_1)$]

$$L_1=\frac{4E_1\pi r_1^2}{3\pi(1-\nu^2)}\left(\frac{h_1}{R_1}\right)^{1/2}$$

and $\pi r_1^2=h_1R_1$ we get

$$h_1=\left(\frac{3(1-\nu^2)L_1}{4E_1R_1^{1/2}}\right)^{2/3}.$$

Thus

$$\begin{aligned}l_1^2\sigma_1^2=\frac{L_1^2}{\pi r_1^2}&=\frac{L_1^2}{h_1R_1}\\&=\left(\frac{4E_1}{3(1-\nu^2)R_1}\right)^{2/3}L_1^{4/3}\\&=\left(\frac{4E_1}{3(1-\nu^2)R_1}\right)^{2/3}\left(a^2\sigma_0\frac{3}{2}\right)^{4/3}\left(1-\frac{r^2}{r_0^2}\right)^{2/3}.\end{aligned}$$

Now, note that

$$F=l_0^2\sigma_0^2\,\mathrm{Im}\left(\frac{1}{E(\omega_0)}\right)+\int d^2x\, n l_1^2\sigma_1^2\,\mathrm{Im}\left(\frac{1}{E(\omega_1)}\right). \quad \text{(A1)}$$

Using (A1) and that $L_0=\sigma_0 l_0^2$ gives

$$\begin{aligned}\mu=&\sigma_0\,\mathrm{Im}\left(\frac{1}{E(\omega_0)}\right)\\&+\frac{3}{5}\left(\frac{3a}{(1-\nu^2)R_1}\right)^{2/3}E_1^{2/3}\sigma_0^{1/3}\,\mathrm{Im}\left(\frac{1}{E(\omega_1)}\right). \quad \text{(A2)}\end{aligned}$$

Now, according to Hertz contact theory

$$\sigma_0=\left(\frac{4E_0}{3(1-\nu^2)R_0}\right)^{2/3}L_0^{1/3}.$$

Substituting this in (A2) would give a friction coefficient which depend on the load, which is usually not observed experimentally. However, as discussed in Sec. III B, if we assume a distribution of heights for the (big) surface asperities, then the average stress σ_0 will be (nearly) independent of the load and of the number of surface asperities: $\sigma_0\approx C_0E_0$. Using this result (note: there is a difference by a factor of order unity between the average of $\langle\sigma_0\rangle^{1/3}$ and $\langle\sigma_0^{1/3}\rangle$; this difference is irrelevant for the present discussion) in (A2) gives

$$\mu=C_0\frac{\mathrm{Im}\,E(\omega_0)}{|E(\omega_0)|}+C_1\frac{\mathrm{Im}\,E(\omega_1)}{|E(\omega_1)|}, \quad \text{(A3)}$$

where

$$C_1 = \frac{3}{5}\left(\frac{3a}{(1-\nu^2)R_1}\right)^{2/3}\left(\frac{|E(\omega_0)|}{|E(\omega_1)|}\right)^{1/3} C_0^{1/3}. \tag{A4}$$

[1] D. F. Moore, *The Friction and Lubrication of Elastomer* (Pergamon, Oxford, 1972); M. Barquins, Mater. Sci. Eng. **73**, 45 (1985); A. D. Roberts, Rubber Chem. Technol. **65**, 673 (1992).

[2] K. A. Grosch, Proc. R. Soc. London, Ser. A **274**, 21 (1963). See also, A. D. Roberts, Rubber Chem. Technol. **65**, 3 (1992); S. P. Arnold, A. D. Roberts, and A. D. Taylor, J. Nat. Rubb. Res. **2**, 1 (1987); M. Barquins and A. D. Roberts, J. Phys. D **19**, 547 (1986).

[3] M. Barquins, Mater. Sci. Eng. **73**, 45 (1985).

[4] B. N. J. Persson, Surf. Sci. **401**, 445 (1998).

[5] B. N. J. Persson, *Sliding Friction: Physical Principles and Applications* (Springer, Heidelberg, 1998).

[6] A. Schallamach, Wear **6**, 375 (1963); Y. B. Chernyak and A. I. Leonov, *ibid.* **108**, 105 (1986).

[7] G. Heinrich, Kautsch. Gummi, Kunstst. **45**, 173 (1992); Rubber Chem. Technol. **70**, 1 (1997).

[8] M. Klüppel and G. Heinrich, Rubber Friction on Self-Affine Road Tracks, Paper No. 43, Meeting of the Rubber Division, American Chemical Society, Chicago, Illinois, April 13–16, 1999.

[9] J. A. Greenwood, in *Fundamentals of Friction, Macroscopic and Microscopic Processes*, edited by I. L. Singer and H. M. Pollack (Kluwer, Dordrecht, 1992).

[10] K. Mori *et al.*, Rubber Chem. Technol. **67**, 798 (1994).

[11] J. F. Archard, Proc. R. Soc. London, Ser. A **243**, 190 (1957).

[12] A. Majumdar and B. Bhushan, J. Tribol. **113**, 1 (1991).

[13] B. N. J. Persson, Phys. Rev. Lett. **81**, 3439 (1998); J. Chem. Phys. **110**, 9713 (1999).